Theor Chem Account (2009) 122:77–86
DOI 10.1007/s00214-008-0486-8

REGULAR ARTICLE

A theoretical investigation of intermolecular interaction of a phthalimide based "on–off" sensor with different halide ions: tuning its efficiency and electro-optical properties

Shabbir Muhammad · Chunguang Liu · Liang Zhao · Shuixing Wu · Zhongmin Su

Received: 21 August 2008 / Accepted: 29 September 2008 / Published online: 22 October 2008

Abstract The interaction between chemosensor, *N*-(2-methyl-1,3-dioxo-indan-5-yl)-benzamide (**1**) and different halide ions (F^-, Cl^- and Br^-) has been investigated using density functional theory (DFT). A clear insight of the sensor anion binding process has been presented. Our calculations revealed that the observed colorimetric and fluorescent signals are induced due to the ground state deprotonation of the sensor molecule caused by F^- which has two times higher binding affinity than other halide ions (Cl^- and Br^-). Derivatives of system **1** have been made to find a better sensor with higher binding affinity and longer wavelength of absorption. All the derivatives are better sensors than the parent **1** except 4-methyl-*N*-(2-methyl-1,3-dioxo-indan-5-yl)-benzamide (**2**). Among these derivatives, trimethyl-[4-(2-methyl-1,3-dioxo-indan-5-ylcarbamoyl)-phenyl]-ammonium (**8**) and (5-benzoylamino-1,3-dioxo-indan-2-yl)-trimethyl-ammonium (**9**) showed a change to higher binding energies of about 58 Kcal/mol and longer absorption wavelengths of 53 nm after deprotonation process than the parent system **1** which is highly demanded in selective chemical sensing. Systems **8**, **9** and their deprotonated zwitterionic forms (**8z** and **9z**) have also been studied for their nonlinear optical responses. Systems **8**, **9** showed significantly good first hyperpolarizability (β) of 84×10^{-30} and 40×10^{-30} esu, respectively. These β values increase in zwitterionic states up to 216×10^{-30} and 109×10^{-30} esu, respectively after deprotonation with F^-, representing a new signal of deprotonation.

Keywords Halide ions · Chemosensor · Deprotonation · Nonlinear optical responses · Zwitterionic states · First hyperpolarizability

1 Introduction

A chemical sensor is a molecule that transforms chemical information into an analytically useful signal [1]. A significant amount of work has been devoted to obtain specific sensors that are able to change, one or several macroscopic properties upon addition of target species. The reason for this intensive interest is the importance of the detection and quantification of anions in disciplines such as biology and environmental sciences [2]. Among the interests in biologically functional anions, fluoride ion has the particular importance because of its association with nerve gases, the analysis of drinking water, refinement of uranium used in nuclear weapons manufacture, established role in dental care and treatment of osteoporosis [3, 4]. Being the smallest and the most electronegative atom, fluoride ion has unique chemical properties and can form the strongest hydrogen-bond interaction with hydrogen-bond donors. The majority of the reported fluoride sensors are based on both colorimetric and fluorescent changes [5, 6]. Many fluorescent sensors have been developed on the basis of a variety of signaling mechanisms such as competitive binding [7], photoinduced electron transfer [8], metal-ligand charge transfer [9], intermolecular excited state proton transfer (IESPT) [10], intramolecular charge transfer [11] and intermolecular proton transfer (IPT) [12]. IPT is a commonly utilized method in designing new anion

Electronic supplementary material The online version of this article (doi:10.1007/s00214-008-0486-8) contains supplementary material, which is available to authorized users.

S. Muhammad · C. Liu · L. Zhao · S. Wu · Z. Su (✉)
Institute of Functional Material Chemistry,
Faculty of Chemistry, Northeast Normal University,
130024 Changchun, People's Republic of China
e-mail: zmsu@nenu.edu.cn

sensors due to the simplicity of its mechanism [13–16]. Recently, Liu et al. [3] reported a naphthalimide containing fluorescent chemosensor for fluoride, based on IPT signaling. However, the details about the anion recognition, have not been disclosed, and consequently the relationship between the selectivity and the molecular structure is still not clear. Similarly, Boiocchi et al. [17] have investigated various chromophores containing hydrogen bonded sites and concluded that the deprotonation trend has enhanced by the increase of the acidity of the hydrogen bond donors.

A significant amount of experimental work has already been reported to obtain specific chemosensors [3–18]. But still there is hardly any detailed theoretical study that can help in understanding the recognization process of these newly synthesized sensor molecules [19, 20]. In designing the new sensor molecules, it is difficult to detect and amplify an anion binding event to produce a measurable output signal [21–24]. This can be made simple with a detailed insight into the sensor anion interactions, which is currently possible through an efficient quantum chemical study on these systems. Taking all these aspects into consideration, a comprehensive DFT study has been carried out on a recently synthesized, both colorimetric and fluorescent fluoride ion chemosensor **1** [25]. In this study, special emphasis has been given to sensor-anion interactions and its signaling properties. In addition to this, we checked the possibility of substitutions of electron donating and withdrawing groups on the sensor to improve its output signaling properties and binding affinity for better efficiency.

2 Computational details

Calculations were performed using Gaussian03 program [26]. All geometry optimizations of neutral molecules and their deprotonated ions for ground state (S_o) were performed using Becke's exchange functional [27], combined with Lee–Yang–Parr correlation functional [28] and denoted as B3LYP [29]. Extensive literature study shows that B3LYP yields accurate results for calculating binding energies in H-bonded systems. It has been asserted that B3LYP is good (although not the best) functional for H-bonding interactions through its comparison with the second-order Moller-plesset (MP2) and experimental data [19, 20, 30–35]. First excited singlet state (S_1) structures for neutral **1** and $\mathbf{1}^-$ (deprotonated anion of **1**) were optimized by CIS [36] method. UV–Vis absorption and fluorescent properties of **1**, $\mathbf{1}^-$ and the derivatives of **1** were calculated by TD-B3LYP [37, 38] method. The spectra were also calculated by TD-B3LYP method considering solvent effects with dielectric constant value of acetonitrile through conductor polarizable continuum model (CPCM) [39] using the cavity parameters as suggested by Klamt, i.e. the approach of conductor-like screening model for real solvent CPCM (COSMO) [40]. All ground state optimizations have been performed using 6-31G* basis set. For TD-B3LYP and CIS besides 6-31G* basis set 6-31 + G* basis sets has also been employed for checking the effect of diffuse functions. Similarly, binding energies has also been calculated at both 6-31G* and 6-31 + G* basis sets. Furthermore, three $\mathbf{1X}^-$ (X = F, Cl, Br) complexes of system **1** were optimized at B3LYP/6-31G* in gas phase, solvent and with basis set superimposition error (BSSE). As above mentioned CPCM (COSMO) is only available for single point calculations in Gaussian 03, we used polarized continuum method (PCM) [41] and Onsager method [42] for optimization of these complexes using the dielectric constant value of acetonitrile as solvent. Onsager method of self-consistent reaction field (SCRF) with a spherical shape cavity is based on the Onsager model that has reproduced comparable results with PCM and experiment data in certain reports [43]. Onsager calculations require values of the molecule volume besides the dielectric constant. This volume was calculated by using the volume keyword for each system before Onsager calculations. PCM model assumes that the solvent is a continuum dielectric, which generates a reaction field interacting with the solute charge distribution.

In intermolecular interactions, basis functions centered at one molecule help to compensate the basis set incompleteness on the other molecule leading to overestimation of binding energy. BSSE will be zero if complete basis sets are used (which is impossible in practice). Counterpoise (CP) correction scheme of Boys–Bernardi [44] has been used to take into account of BSSE. This method has been used to calculate the binding energies of sensor halide ion complexes considering sensor molecule as fragment A and halide ion as fragment B using the following equation:

$$\mathrm{De}_{\mathrm{BSSE}}(\mathrm{AB}) = E\left(\mathrm{AB}^{\mathrm{AB}}\right) - E\left(\mathrm{A}^{\mathrm{AB}}\right) - E\left(\mathrm{B}^{\mathrm{AB}}\right) \quad (1)$$

where $E(\mathrm{AB}^{\mathrm{AB}})$ is the energy of the complex AB with the basis set of AB, while $E(\mathrm{A}^{\mathrm{AB}})$ and $E(\mathrm{B}^{\mathrm{AB}})$ are the energies of fragment A and fragment B, respectively, with the basis set of AB at their respective geometries adopted from the complex of AB.

3 Molecular geometries

On Sarkar's [25] work a further important point about the structure of system **1** has been found. They presented a gas phase structure of **1** in which the benzoyl group is bent over the pthalimide part. In our study, we further investigated about structure using a more accurate basis set, i.e. 6-31G* and found a minimum potential energy surface in which

both parts instead of bending over each other they are in some what linear fashion as shown in Scheme 1. To find the global minimum between these two forms, both the structures were optimized with the same method and basis set. It was found that linear structure has lower energy and more stable than its bent form. After checking the frequency calculations, we performed additional single-point calculations at higher basis set, i.e. 6-31 + G**. It was further confirmed that at both levels of theory B3LYP and HF, the linear form is more stable than the bent form by 4.43 and 4.55 Kcal/mol, respectively. So we used linear form in rest of our computational work.

4 Selectivity of fluoride ion

For an excellent chemosensor, high selectivity is considered as a matter of importance. The calculated binding energies for the complexes formed between hydrogen bond donors and acceptors provide a useful scale to assess the relative strengths of these interactions. In many studies, binding energies have been successfully correlated with the selectivity in anion sensing processes [45–49]. While in some others cases these have also been found in good agreement with experimentally calculated association constants [19, 49]. To check the selectivity trend of previous experimental work, we have calculated binding energies of **1** and the halide ions. The binding energies (De) of complexes $\mathbf{1}\cdot F^-$, $\mathbf{1}\cdot Cl^-$ and $\mathbf{1}\cdot Br^-$ have been calculated by considering the BSSE (Table 1). The calculated binding energy of fluoride complex supports the distinct selectivity of fluoride ion from the other halides. At both levels, B3LYP/6-31G* and B3LYP/6-31 + G*, the binding energies of $\mathbf{1}\cdot F^-$ are −74.81 and −54.28 Kcal/mol, respectively which are more than twice as those of $\mathbf{1}\cdot Cl^-$ and $\mathbf{1}\cdot Br^-$. The fluoride ion has high electronegativity and smaller size; it reacts more vigorously to the acidic proton of chemosensor molecule (**1**) as compared

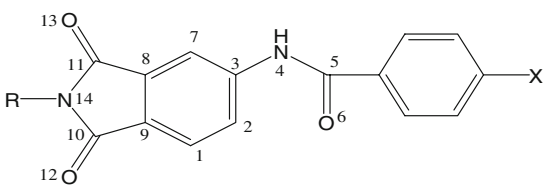

Parent 1 : R = CH_3, X = H

Derivatives

2 : R = CH_3, X = CH_3 3 : R = CH_3, X = CN

4 : R = CN , X = H 5 : R = CH_3, X = NO_2

6 : R = NO_2, X = NO_2 7 : R = NO_2, X = H

8 : R = CH_3, X = $\overset{+}{N}R_3$ 9 : R = $\overset{+}{N}R_3$, X = H

Scheme 1 Labeled structure of **1** molecule and its derivatives

Table 1 Calculated BSSE corrected binding energies De_{BSSE} (Kcal/mol)

Basis sets	Energy	$\mathbf{1}\cdot F^-$	$\mathbf{1}\cdot Cl^-$	$\mathbf{1}\cdot Br^-$
6-31G*	De_{BSSE}	−74.81	−32.17	−29.11
6-31 + G*	De_{BSSE}	−54.28	−29.78	−25.40

with other halide ions (Cl^-, Br^-) leading the abstraction of its proton (explained in next Sect. 5). This trend found in our calculations correlates well with already calculated binding energies of different halide ions through this method and experimental work [19, 25, 49].

5 Proton abstraction

In order to further investigate, either the recognization process is mediated through the H-bonding interaction (N–H:::F) between **1** and F^- or proton abstraction (PA) (N:::H–F) from the amido hydrogen of **1** to F^-, the three complex systems consist of $\mathbf{1}X^-$ (X = F, Cl, Br), with an initial H···X distance set at around 1.75Å (as a typical N···HX hydrogen bond distance ranging from 1.73 to 1.77Å) and NH···X angles >110° [50, 51] have been optimized. The most important bond parameters for these complexes that were optimized with, without BSSE correction and also in a continuum medium have shown in Table 2.

As BSSE is considered important especially in weak intermolecular interactions where it has shown close agreements with experimental results [52, 53], we selected the BSSE optimized geometry to differentiate between hydrogen bonding (HB) and PA. Comparing the N–H bond length of $\mathbf{1}\cdot F^-$ with **1** molecule it is clear that N–H bond has broken in the optimized complex wherein N–H distance is 1.801Å (instead of a normal N–H distance of 1.01 Å). From the change of N–H distance (greater than 0.790 Å) it is clear that the N–H bond has been broken and H^+ moved close to F^- with $R_{H\cdots F} = 0.96$ Å in $\mathbf{1}\cdot F^-$ complex (Fig. 1). For further confirmation of this PA, Wiberg bond indices and natural atomic charges were calculated at the BSSE optimized geometries by using the natural bond orbital (NBO) analysis option as incorporated in the Gaussian 03 program and are presented in Table 3.

A careful analysis of Table 3 shows that among these halide ions only F^- has considerably lowered its negative charge with a concurrent increase at N atom of amido group. This is of course, due to the abstraction of amido proton from N atom (gain −ve charge) while it is not in the case of Cl^- and Br^-. A similar conclusion can be obtained by examining the results of Wiberg bond indices in Table 3 where bond indices of N, H and X atoms show the formation of N:::H–X^- specie in $\mathbf{1}\cdot F^-$ complex with a bond index of 0.594

Table 2 Bond distances (Å) of RH–N and RH–X and H-bond angles (°) of $\theta_{N-H\cdots X}$, $\Phi_{C5-N-H\cdots X}$ in $\mathbf{1}X^-$ optimized complexes with different methods

Method	Complexes	R_{N-H}	$R_{H\cdots X}$	$\theta_{N-H\cdots X}$	$\Phi_{C5-N-H\cdots X}$
Without BSSE	$\mathbf{1}\cdot F^-$	1.471	1.032	171.51	46.84
	$\mathbf{1}\cdot Cl^-$	1.040	2.220	168.23	0.18
	$\mathbf{1}\cdot Br^-$	1.044	2.414	167.92	0.04
	1	1.010	–	–	–
With BSSE	$\mathbf{1}\cdot F^-$	1.801	0.968	172.90	63.20
	$\mathbf{1}\cdot Cl^-$	1.040	2.216	168.71	1.57
	$\mathbf{1}\cdot Br^-$	1.037	2.434	168.46	1.85
With soln.					
Onsager	$\mathbf{1}\cdot F^-$	1.462	1.038	171.72	38.63
	$\mathbf{1}\cdot Cl^-$	1.032	2.345	168.90	0.10
	$\mathbf{1}\cdot Br^-$	1.031	2.501	168.24	0.30
PCM	$\mathbf{1}\cdot F^-$	1.130	1.342	169.72	25.49
	$\mathbf{1}\cdot Cl^-$	1.021	2.532	166.07	0.33
	$\mathbf{1}\cdot Br^-$	1.021	2.677	166.00	0.63

between F and H atoms while a weak H-bond interaction N–H:::X^- have been observed in $\mathbf{1}\cdot Cl^-$ and $\mathbf{1}\cdot Br^-$ complexes with bond indices of 0.110 and 0.031, respectively. Our results are in good agreement with the fact that IPT between chemosensor **1** and F^- took place on adding enough amount of tetrabutylammonium fluoride (TBAF) to the sensor's solution, where as it was not in case of Cl^- and Br^- as shown in experimental work [25].

Comparisons between BSSE geometries and PCM optimized geometries of $\mathbf{1}X^-$ complexes show different

Table 3 NBO charges and bond indices of three $\mathbf{1X}^-$ (X = F, Cl, Br) complexes

System	NBO charges		Wiberg bond index	
	N	X	N–H	H–X
$\mathbf{1}\cdot F^-$	−0.716	−0.609	0.102	0.594
$\mathbf{1}\cdot Cl^-$	−0.620	−0.854	0.667	0.110
$\mathbf{1}\cdot Br^-$	−0.619	−0.851	0.680	0.031

trends. In BSSE the increase in N–H distance 0.790 Å supports the PA while in PCM geometry this difference is only 0.120 Å which favors the HB. Although this change in N–H bond length at two other optimized geometries (in gas and Onsager method) is less than at BSSE but their H–F^- bond length is consistent with the H–F average bond length of 1.14 Å in HF_2^- molecule [54] which supports PA. The difference between PCM and other three optimized geometries may be due to difference of methodology to optimize these complexes. Unlike the other three methods, in PCM model the cavity is created via a series of overlapping spheres and hydrogen is treated explicitly from its heavy atom which may lead to the underestimation of this change in N–H and H–F distances in optimization.

6 Absorption and fluorescence spectra

Maximum absorption (λ_{ab}) and emission wavelengths (λ_{em}) of **1** and $\mathbf{1}^-$ are presented in Table 4. These were calculated by TD-B3LYP method using various basis sets and also

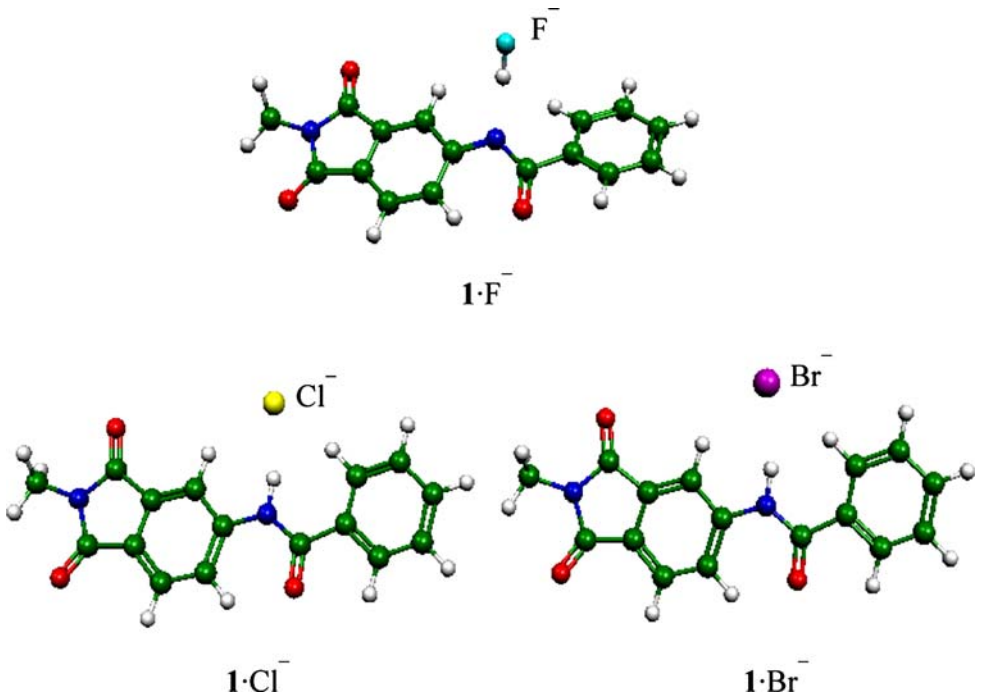

Fig. 1 Optimized complexes of $\mathbf{1}X^-$ (X = F, Cl, Br) with BSSE correction

Table 4 Maximum absorption λ_{ab} (nm) and emission λ_{em} (nm) wavelengths of **1** and its $\mathbf{1}^-$ by TD-B3LYP with different basis sets

Basis set	Absorption wavelengths λ_{ab}		Emission wavelengths λ_{em}	
	1 Neutral	$\mathbf{1}^-$ Deprotonated	**1** Neutral	$\mathbf{1}^-$ Deprotonated
6-31G*	328	455	371 (410)[a]	495 (517)
6-31 + G*	335	468	381 (411)	517 (539)
Experimental[b]	330	425	412	570

[a] Values in parenthesis have taken considering CPCM (COSMO) solvent effect

[b] Experimental results are taken from Ref. [25]

Table 5 According to Scheme 1 labeled atoms, bond lengths (Å), bond angles and dihedral angles (°) in **1** and $\mathbf{1}^-$

Bond lengths	**1** Neutral	$\mathbf{1}^-$ Deprotonated	Bond angles	**1** Neutral	$\mathbf{1}^-$ Deprotonated
N_4–C_3	1.402	1.360	C_2–C_3–N_7	120.2	116.8
N_4–C_5	1.386	1.352	C_2–C_3–N_4	116.7	116.7
C_5–O_6	1.224	1.249	C_7–C_3–N_4	123.0	127.5
C_7–C_8	1.384	1.379	C_3–N_4–C_5	128.8	122.3
C_8–C_{11}	1.497	1.494	N_4–C_5–O_6	123.3	129.8
C_9–C_{10}	1.487	1.462	C_2–C_3–N_7	120.2	116.8
C_{10}–C_{12}	1.215	1.225	C_2–C_3–N_4	116.7	116.7
C_{11}–C_{13}	1.401	1.22	C_7–C_3–N_4–C_5	4.1	0.006
C_{11}–N_{14}	1.402	1.401	C_3–N_4–C_5–O_6	2.8	0.000
C_{10}–N_{14}	1.407	1.422	N_4–C_5-Ph	25.4	0.003
C_{15}–N_{14}	1.452	1.442	O_6–C_5-Ph	22.9	0.004

CPCM (COSMO) solvent effects were included. Both λ_{max} of absorption and emission for **1** and its $\mathbf{1}^-$ are slightly basis sets dependent especially when adding diffuse functions to C, N and O atoms.

CPCM (COSMO) solvent effects are significant for λ_{em} of **1** and $\mathbf{1}^-$. All the calculated λ_{ab} values for **1** and $\mathbf{1}^-$ are in good agreement with the experimental results using 6-31G* basis set. Adding diffuse function showed an overall increase in both absorption and emission wavelengths but the trend is same by comparing the values at both basis sets between neutral and anionic species. For fluorescent λ_{em}, TD-B3LYP/6-31 + G* including bulk acetonitrile solvent effects gives the best converged result for **1**, but for $\mathbf{1}^-$ these basis sets little overestimate. Li et al. [20] using the same method and basis set have calculated the emission spectrum of 4-benzoylimido-*N*-butyl-1-8-naphthalimide anion with a difference of 51 nm to the experimental value. They described this difference due to the neglect of solvent effect on the geometry optimization of anionic structure but in our case with a similar anion and method the difference is just 31 nm which can be easily rationalized with reference to the above work reported previously. Simulation of both absorption and fluorescence spectra observed in experiment give credit to the choice of calculation method [25].

It has been also investigated that the observed colorimetric and fluorescent signals are induced due to the sensor's deprotonation by F^-. The deprotonation of amido hydrogen causes a significant increase of electron charge density on nitrogen atom of amido group associated with enhanced push–pull character between amido and carbonyl groups [55, 56]. Besides this, comparing the geometry of system **1** neutral molecule with its anionic structure after deprotonation, it is found that the π conjugation becomes extensive in $\mathbf{1}^-$ than **1**. The bond lengths of N_4–C_3, N_4–C_5, C_9–C_{10}, and C_8–C_{11} (Table 5) are shortened more significantly than others, suggesting the stronger coupling among amido, benzene ring and carbonyl groups in $\mathbf{1}^-$. This is further confirmed by the dihedral angles between phthalimide, amido and benzoyl components that have become almost zero resulting a planar structure and easy redistribution of charge during excitation. As a consequence, the HOMO-LUMO energy gap decreased in host sensor molecule after deprotonation by an external F^-. The lower HOMO-LUMO energy gap implies that it is easier to promote an electron from the ground state to excited state which is in accordance with the observed red-shifted in absorption and emission wavelengths of deprotonated anion (Scheme 2).

7 Tuning of sensor molecule

The emission color of a fluorescent sensor is important in selective detection because it is often needed to avoid probable interferences by the fluorescence impurities

Scheme 2 Schematic representation of system **1** deprotonation process for F^-

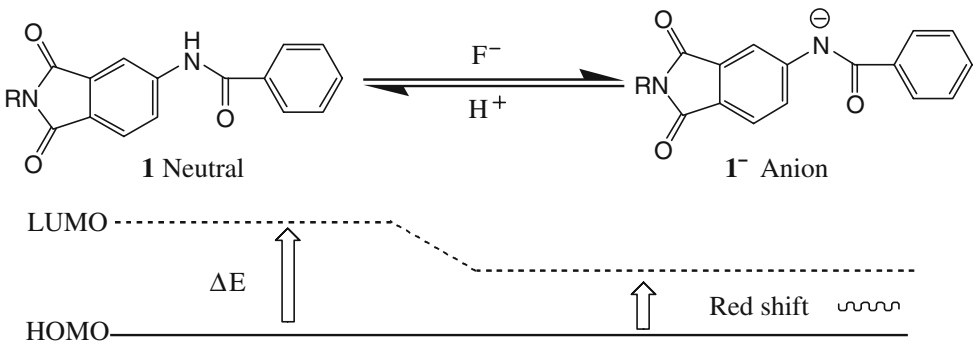

present in environmental and biological samples. In spite of several efforts, in modifying the emission color of sensor molecule still theoretical methods based on molecular orbital calculations have scarcely been exploited [32].

For selective detection, a sensor with higher binding affinity and longer wavelength of absorption and emission is desired. We tuned these two important properties of sensor, i.e. its binding affinity with F^- that can be increased by making the sensor molecule as stronger electron acceptor. For achieving a change in wavelength, it is well known that by adding the electron-donating or withdrawing groups to fluorophores generally cause changes in their transition energies consistent with a shift not only in absorption but also in emission wavelength. The pristine sensor molecule **1** shows a maximum absorption wavelength at 330 nm and has calculated binding energy of −74.81 Kcal/mol with F^- (see Table 8 in supporting information). Therefore, as novel F^- sensors derivatives of **1** having absorption maximum at a longer wavelength and higher binding energies than that of **1** are desired in chemical sensing. For checking the effect of substituents, we selected two positions (N-phthal and para benzoyl) on system **1** molecule as shown in Scheme 1. From experimental standpoint, N-phthal nitrogen atom of phthalimide is more favorable for many kinds of reactions due to the alpha position to the both carbonyl groups [57, 58]. But benzoyl ring has three possible positions, i.e. ortho, meta and para. These three positions have been checked systematically and selected the para position due to its higher stability and less steric hindrances in derivative molecules. So these two positions for substitutions have been taken, i.e. N-phthal and para benzoyl of system **1**. Figure 2 presents change in binding energy with different withdrawing groups, i.e. CN, NO_2 and NR_3^+ at these two selected positions. These groups showed higher binding energies at N-phthal position than their counter benzoyl positions due to the carbonyl groups at phathal position that add up to their withdrawing effects but in case of stronger withdrawing groups this effect becomes less distinct (Fig. 2).

It is also noticed that in case of system **2**, methyl group being a poor electron releasing could not produce any

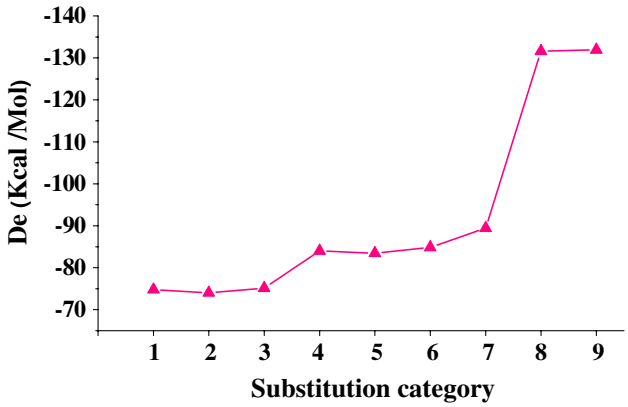

Fig. 2 Plot of BSSE corrected binding energies (De) of system **1** and its derivatives

significant change both in binding energy and absorption maximum (see Table 8 in supporting information). To obtain a reliable spectrum data of substitutions, besides B3LYP we have also employed PBE0 [59] functional which embodies a different percentage of exact exchange than B3LYP. Both methods show a good consistent trend in calculating the transition energies of substitutions presented in Fig. 3. Although the addition of diffusion functions showed higher absorption wavelengths but the over all trend among different substituents is about same (Fig. 3). So in this comparative type of study the results of both the basis sets could be consider reliable. Figure 3 shows that NO_2 group derivatives have considerably increased λ_{max} as compared with parent system **1** and CN derivatives. This might be due to NO_2 group which joins molecular conjugation at benzoyl position and extends the conjugated-system of sensor and its anion. In system **8** and **9,** besides a strong inductively withdrawing group NR_3^+ has a formal positive charge which also produces some electrostatic interactions in sensor. Both the substitutions are more effective than CN and NO_2 derivatives in producing higher binding energy and longer wavelength of absorption and show the binding energy of about 132 Kcal/mol twice the parent system **1** and a red shift of 58 nm absorption

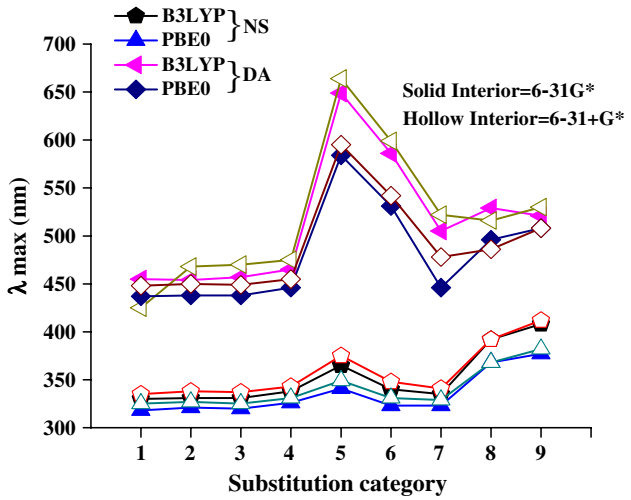

Fig. 3 Plot of calculated absorptions of different substituents of sensor **1** for neutral sensors (NS) and their deprotonated anions (DA)

maximum in deprotonation process. After deprotonation with F^- system **8** and **9** produce zwitterions. Amendola et al. [60] have also determined the efficiency of an amide based receptor which formed zwitterions after deprotonation with F^-. Besides this, they have successfully isolated the zwitterions as a crystalline solid. From this, we can rationalize the efficiency and reliability of our predicted **8** and **9** derivatives. Thus in short, our substitutions can predict not only a higher absorption and emission wavelengths but also a sensor molecule with higher anion binding affinity that is highly desirable in selective sensing.

8 First hyperpolarizability

Ionic and zwitterionic organic chromophores are considered to be an important new class of materials for application in nonlinear optics. Polar molecules can be utilized in poled polymers where large dipole moments (μ) play an important role [60]. Currently, there is a need to develop molecules with large dipole and hyperpolarizability values for poled polymers as they seem to be closest to commercial applications [61, 62]. Lambert et al. [63] have studied a new family of zwitterionic NLO chromophores in which a polyene bridge is capped by phenyl rings substituted by NR_3^+ at one end and at the other end by BR_3^+. Abbotto et al. [64, 65] have also reported the synthesis and NLO properties of a series of novel zwitterionic chromophores. Their measured $\mu\beta$ values are negative and one of the highest values reported till now in the literature. Hyperpolarizabilities are often described within the dipolar approximation on the basis of the so-called two-state model [66]. Within the frame work of two state model the β value is expressed as

$$\beta_\mu(0) = \frac{3(M_{ge})^2 \Delta\mu}{2(\hbar\omega_{ge})^2}$$

where $\Delta\mu = \mu_e - \mu_g$ is the difference between the dipole moments in the excited and ground states, $\hbar\omega_{ge}$ is the transition energy, and M_{ge} is transition dipole moment between the ground and excited states. Hence the two level model requires that a well-performing NLO chromophore possess a low energy CT excited state with large oscillator strength. In above studied derivatives, systems **8**, **9** and their deprotonated forms (**8z** and **9z**) are ionic and zwitterionic chromophores, respectively with high dipolar characters in their ground states. Zwitterionic system 8z and 9z show a significantly higher ground state dipole moment and lower transition energy than system **8** and **9**. Many similar zwitterionic systems have shown good NLO response with these properties [67, 68] that inspired us to probe into the NLO responses of these four systems. The first hyperpolarizability (β) was calculated by using time-dependent density functional theory (TDDFT) combined with the sum-over-states (SOS) method. Our group has successfully applied this method to investigate the NLO properties of a series of compounds [65–72]. First 50 excited states were calculated using TD-B3LYP model. Then those physical values were taken as input of the SOS formula to calculate the β value. The accuracy of SOS methods mainly depends on the convergence of calculation results.

The plot of β_{vec} values versus the number of excited states involved in SOS formalism for the studied compounds has represented in Fig. 4. It can be seen that the convergences are stable after summation over about 40 states for all studied compounds except system **8** for which we took 100 excited states. Accordingly, it is a reasonable approximation in the calculation of β_{vec} by employing 50

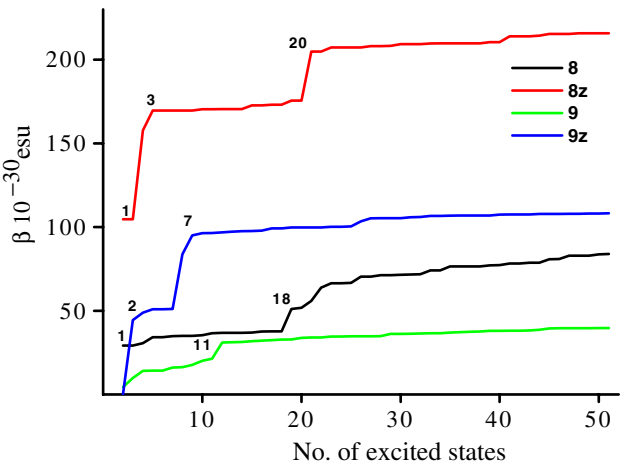

Fig. 4 Plot of β values versus the number of excited states of studied system

excited states in the SOS method in this work. Although 27 components of β tensor can be computed but the components along the direction of dipole moment are taken as β_{vec}. Thus β_{vec} is defined as

$$\beta_{\mu} = \beta_{vec} = \sum_{i=1}^{3} \frac{\mu i \beta i}{\mu}, \quad (2)$$

where μ is ground state dipole moment and

$$\beta_i = \beta_{iii} + 1/3 \sum_{i \neq j} \left(\beta_{jii} + \beta_{iji} + \beta_{iij}\right), \quad i,j = (x,y,z) \quad (3)$$

Because the x-axis is directed along the axis of charge transfer in our studied systems as shown in Fig. 5 of supporting information, so in our calculations the largest component of the β is also β_{xxx} (Table 6).

All other components have small values, thus $\beta_{vec} \approx \beta_{xxx}$. The β_{vec} of these systems consider in this study were calculated under the external electronic field and the laser frequency of $\omega = 0.65\,\text{eV}(\lambda = 1,907\,\text{nm})$. From Table 6, we can see β_{vec} of above systems are determined by β_{xxx}. To gain an insight into the hyperpolarizabilities of studied systems TD-DFT calculations have been carried out. The transition energy, oscillator strengths and major contribution of crucial transitions for all systems are listed in Table 7 along with their orbital features. Here the crucial transitions are those who have major contribution to the value of β_{xxx} and can be seen in Fig. 4. The TD-DFT results indicate the contributions of these crucial transitions are in additive fashion so we studied more than one transition. Both the system **8** and **8z** show higher β_{vec} values than **9** and **9z** that can be attributed to their lower $\hbar\omega_{ge}$ values. The similar trend can also be seen from going protonated forms (**8** and **9**) to deprotonated zwitterionic forms (**8z** and **9z**) where higher $\left(M_{ge}\right)^2$ and lower $\hbar\omega_{ge}$ values lead to the larger β_{vec} of **8z** and **9z**. Another factor about higher β_{vec} of **8z** is that it has contributions from three low energy crucial transitions while that is not the case with other NLO studied systems.

For example **8z** have highest β_{vec} among the studied systems with its two low energy transitions from HOMO to LUMO and HOMO-2 to LUMO. It can be seen that electron densities of HOMO and HOMO-2 are largely on phthalimide and amido parts while LUMO is heavily located towards the withdrawing group NR_3^+. Similar CT features of frontier molecular orbitals (FMO) during excitations can also be seen in other studied systems but the worth of charge transfer is less extensive than **8z**. These calculated β_{vec} values are several times higher than those of typical compounds containing highly push–pull groups, e.g. the calculated β_{vec} value of system **8** is about 6 times higher than the average β of the para nitro aniline (PNA) [73] calculated with same method and external field strength. It is interesting to note that in going from protonated forms to zwitterionic both derivatives show a remarkable increase in their β_{vec} that becomes 216×10^{-30} and 109×10^{-30} esu for **8z** and **9z**, respectively (Table 6).

The difference of β_{vec} between protonated and their zwitterionic forms can be further enhanced by either improving delocalization or increasing the strength of donor or acceptor groups (improving electron asymmetry). So in this way besides F^- sensor these can also be used as NLO materials and in NLO switching induced by F^-.

Table 6 Second order nonlinear optical coefficients of systems **8**, **8z**, **9** and **9z**

System no.	μ (Debye)	β_{xxx} (10^{-30} esu)	β_{vec} (10^{-30} esu)
8	18.77	84.47	83.88
8z	29.20	215.65	215.77
9	11.29	39.47	39.64
9z	15.96	108.23	109.25

Table 7 Excited states contributions to β for studied molecules calculated by TD-DFT

Compound	Excited states	$\left(M_{ge}\right)^2$	$\hbar\omega_{ge}$	f_{os}	Major transitions	c_i
8	$S_0 \rightarrow S_1$	2.128	3.157	0.168	$H \rightarrow L$	0.45
	$S_0 \rightarrow S_{18}$	2.902	5.088	0.412	$H-2 \rightarrow L+2$	0.45
8z	$S_0 \rightarrow S_1$	3.358	2.340	0.193	$H \rightarrow L$	0.64
	$S_0 \rightarrow S_3$	2.548	2.687	0.168	$H-2 \rightarrow L$	0.48
	$S_0 \rightarrow S_{20}$	5.089	4.673	0.600	$H-2 \rightarrow L+2$	0.67
9	$S_0 \rightarrow S_{11}$	4.769	4.769	0.568	$H-2 \rightarrow L+1$	0.44
9z	$S_0 \rightarrow S_2$	2.709	2.378	0.172	$H \rightarrow L+1$	0.67
	$S_0 \rightarrow S_7$	5.286	3.519	0.500	$H \rightarrow L+1$	0.60

9 Conclusions

The present DFT calculations on a phthalimide based chemosensor provide the theoretical frame work through which the following conclusions can be obtained.

(1) The sensor anion binding is a ground state deprotonation mediated through HB interaction. The calculated binding energies show the stronger affinity of F^- than Cl^- and Br^- and this selectivity trend is in accordance with experiment.
(2) As compared with other halide ions (Cl^- and Br^-), F^- considerably lowers its negative charge after abstraction of a proton from the sensor molecule.
(3) The large red shift of signal is induced by the increase of molecular conjugation and donor strength when sensor is deprotonated by an external F^-.

(4) Our investigation shows that substitutions based on DFT calculations can help not only to improve selectivity but also the binding affinity of such kind of chemical sensors. So using the efficient tool of DFT calculations, we can improve the efficiency of F^- chemosensors that have higher absorption and emission wavelengths but weak binding affinity and vice versa.

(5) First hyperpolarizability calculations of systems **8**, **9**, **8z** and **9z** also show their possibility of molecular NLO switching ability induced by F^-.

Acknowledgments The authors acknowledge the financial support from the National Natural Science Foundation of China (Project Nos. 20573016), Training Fund of NENU'S Scientific Innovation Project (NENU-STC07017) and Science Foundation for Young Teachers of Northeast Normal University (20070304), and are supported by Program for Changjiang Scholars and Innovative Research Team in University (PCSIRT). S.Muhammad also acknowledges Ministry of Education, Pakistan and China scholarship council (CSC) for the award of scholarship in Ph.D. program.

References

1. Hulanicki A, Glab S, Ingman F (1991) Pure Appl Chem 63:1247. doi:10.1351/pac199163091247
2. Stibor I, Zlatuskova P (2005) Chiral recognition of anions. Anion Sens 255:31
3. Liu B, Tian H (2005) J Mater Chem 15:2681. doi:10.1039/b501234a
4. Kleerekoper M (1998) Endocr Metab Clin 27:441. doi:10.1016/S0889-8529(05)70015-3
5. Cho EJ, Ryu BJ, Lee YJ, Nam KC (2005) Org Lett 7:2607. doi:10.1021/ol0507470
6. Thiagarajan V, Ramamurthy P, Thirumalai D, Ramakrishnan VT (2005) Org Lett 7:657. doi:10.1021/ol047463k
7. Niikura K, Metzger A, Anslyn EV (1998) J Am Chem Soc 120:8533. doi:10.1021/ja980990c
8. Gunnlaugsson T, Ali HDP, Glynn M, Kruger PE, Hussey GM, Pfeffer FM, dos Santos CMG, Tierney J (2005) J Fluoresc 15:287. doi:10.1007/s10895-005-2627-y
9. Lin ZH, Zhao YG, Duan CY, Zhang BG, Bai ZP (2006) J Royal chem Soc 3678
10. Choi K, Hamilton AD (2001) Angew Chem Int Ed 40:3912. doi:10.1002/1521-3773(20011015)40:20<3912::AID-ANIE3912>3.0.CO;2-R
11. Wallace KJ, Belcher WJ, Turner DR, Syed KF, Steed JW (2003) J Am Chem Soc 125:9699. doi:10.1021/ja034921w
12. Amendola V, Esteban-Gomez D, Fabbrizzi L, Licchelli M (2006) Acc Chem Res 39:343. doi:10.1021/ar0501951
13. Boiocchi M, Del Boca L, Gomez DE, Fabbrizzi L, Licchelli M, Monzani E (2004) J Am Chem Soc 126:16507. doi:10.1021/ja045936c
14. Boiocchi M, Del Boca L, Esteban-Gomez D, Fabbrizzi L, Licchelli M, Monzani E (2005) Chem Eur J 11:3097. doi:10.1002/chem.200401049
15. Tong H, Zhou G, Wang LX, Jing XB, Wang FS, Zhang JP (2003) Tetrahedron Lett 44:131. doi:10.1016/S0040-4039(02)02504-2
16. Zhang X, Guo L, Wu FY, Jiang YB (2003) Org Lett 5:2667. doi:10.1021/ol034846u
17. Boiocchi M, Fabbrizzi L, Foti F, Monzani E, Poggi A (2005) Org Lett 7:3417. doi:10.1021/ol050981q
18. Gomez DE, Fabbrizzi L, Licchelli M, Monzani E (2005) Org Biomol Chem 3:1495. doi:10.1039/b500123d
19. Hirano J, Hamase K, Zaitsu K (2006) Tetrahedron 62:10065. doi:10.1016/j.tet.2006.08.060
20. Li Z, Zhang JP (2006) Chem Phys 331:159. doi:10.1016/j.chemphys.2006.10.017
21. Neumann T, Dienes Y, Baumgartner T (2006) Org Lett 8:495. doi:10.1021/ol052911p
22. Hudnall TW, Melaimi M, Gabbaı FP (2006) Org Lett 8:2747. doi:10.1021/ol060791v
23. Liu XY, Bai DR, Wang S (2006) Angew Chem Int Ed 45:5475. doi:10.1002/anie.200601286
24. Wiskur SL, Floriano PN, Anslyn EV, McDevitt JT (2003) Angew Chem Int Ed 42:2070. doi:10.1002/anie.200351058
25. Sarkar M, Yellampalli R, Bhattacharya B, Kanaparthi RK, Samanta A (2007) J Chem Sci 119:91. doi:10.1007/s12039-007-0015-7
26. Frisch MJ, Trucks GW, Schlegel HB, Scuseria GE, Robb MA, Cheeseman JR, Montgomery JA Jr, Vreven T, Kudin KN, Burant JC, Millam JM, Iyengar SS, Tomasi J, Barone V, Mennucci B, Cossi M, Scalmani G, Rega N, Petersson GA, Nakatsuji H, Hada M, Ehara M, Toyota K, Fukuda R, Hasegawa J, Ishida M, Nakajima T, Honda Y, Kitao O, Nakai H, Klene M, Li X, Knox JE, Hratchian HP, Cross JB, Bakken V, Adamo C, Jaramillo J, Gomperts R, Stratmann RE, Yazyev O, Austin AJ, Cammi R, Pomelli C, Ochterski JW, Ayala PY, Morokuma K, Voth GA, Salvador P, Dannenberg JJ, Zakrzewski VG, Dapprich S, Daniels AD, Strain MC, Farkas O, Malick DK, Rabuck AD, Raghavachari K, Foresman JB, Ortiz JV, Cui Q, Baboul AG, Clifford S, Cioslowski J, Stefanov BB, Liu G, Liashenko A, Piskorz P, Komaromi I, Martin RL, Fox DJ, Keith T, Al-Laham MA, Peng CY, Nanayakkara A, Challacombe M, Gill PMW, Johnson B, Chen W, Wong MW, Gonzalez C, Pople JA (2004) Gaussian 03, Revision C.02 Gaussian Inc Wallingford CT
27. Becke AD (1993) J Chem Phys 98:5648. doi:10.1063/1.464913
28. Lee C, Yang W, Parr RG (1988) Phys Rev B 41:785. doi:10.1103/PhysRevB.37.785
29. Stephens PJ, Devlin FJ, Chabalowski CF, Frisch MJ (1994) J Phys Chem 98:11623. doi:10.1021/j100096a001
30. van der Wijst T, Fonseca Guerra C, Swart M, Bickelhaupt FM (2006) Chem Phys Lett 426:415. doi:10.1016/j.cplett.2006.06.057
31. Park YC, Lee JS (2007) Bull Korean Chem Soc 28:386
32. Haranczyk M, Rak J, Gutowski M, Radisic D, Stokes ST, Bowen KH (2005) J Phys Chem B 109:13383. doi:10.1021/jp050246w
33. Rak J, Skurski P, Simons J, Gutowski M (2001) J Am Chem Soc 123:11695. doi:10.1021/ja011357l
34. Daübkowska I, Rak J, Gutowski M (2002) J Phys Chem A 106:7423. doi:10.1021/jp020947i
35. van Mourik T, Price SL, Clary DC (1999) J Phys Chem A 103:1611. doi:10.1021/jp983337k
36. Foresman JB, Head-Gordon M, Pople JA, Frisch MJ (1992) J Phys Chem 96:135. doi:10.1021/j100180a030
37. Stratmann RE, Scuseria GE, Frisch MJ (1998) J Chem Phys 109:8218. doi:10.1063/1.477483
38. Bauernschmitt R, Ahlrichs R (1996) Chem Phys Lett 256:454. doi:10.1016/0009-2614(96)00440-X
39. Cossi M, Rega N, Scalmani G, Barone V (2003) J Comput Chem 24:669. doi:10.1002/jcc.10189
40. Eckert F, Klamt A (2002) AIChE J 48:369. doi:10.1002/aic.690480220
41. Miertus S, Scrocco E, Tomasi (1981) J Chem Phys 55:117 doi:10.1016/0301-0104(81)85090-2
42. Onsager (1936) J Am Chem Soc 58:1486

43. Rutkowski KS, Melikova SM, Rodziewicz P, Herrebout WA, van der Veken BJ, Koll A (2008) J Mol Struct 880:64. doi:10.1016/j.molstruc.2007.10.026
44. Boys SF, Bernardi F (1970) Mol Phys 19:553. doi:10.1080/00268977000101561
45. Jose DA, Singh A, Das A, Ganguly B (2007) Tetrahedron Lett 48:3695. doi:10.1016/j.tetlet.2007.03.120
46. Johansson P, Abrahamsson E, Jacobsson P (2005) J Mol Struct THEOCHEM 717:215. doi:10.1016/j.theochem.2004.12.021
47. Johansson P, Jacobsson P (2005) Electrochim Acta 50:3782. doi:10.1016/j.electacta.2005.02.062
48. Solimannejad M, Alkorta I, Elguero J (2007) J Mol Struct THEOCHEM 819:136. doi:10.1016/j.theochem.2007.05.037
49. Shang XF, Xu XF, Lin H, Shao A, Lin HK (2007) J Incl Phenom Macro 58:275. doi:10.1007/s10847-006-9154-6
50. Brooks SJ, Evans LS, Gale PA, Hursthouse MB, Light ME (2005) Chem Comm 734
51. Steiner T (2002) Angew Chem Int Ed 41:48. doi:10.1002/1521-3773(20020104)41:1<48::AID-ANIE48>3.0.CO;2-U
52. Domenicano A, Hargittai I (2002) Strength from weakness: structural consequences of weak interactions in molecules, supramolecules, and crystals. Kluwer, Dordrecht, p 286
53. Chen F, Davidson ER (2002) Chem Phys Lett 360:99. doi:10.1016/S0009-2614(02)00807-2
54. Greenwood NN, Earnshaw A (1997) Chemistry of the Elements, 2nd Edition edn. Butterworth-Heinemann, Oxford
55. Peng XJ, Wu YK, Fan JL, Tian MZ, Han KL (2005) J Org Chem 70:10524. doi:10.1021/jo051766q
56. Thiagarajan V, Ramamurthy P (2007) J Lumin 126:886. doi:10.1016/j.jlumin.2007.01.003
57. Chaignon NM, Fairlamb IJS, Kapdi AR, Taylor RJK, Whitwood AC (2004) J Mol Catal A Chem 219:191–199. doi:10.1016/j.molcata.2004.05.008
58. Hu A, Lin W (2005) Org Lett 7:455. doi:10.1021/ol0474812
59. Ernzerhof M, Perdew JP, Burke K (1997) Int J Quantum Chem 64:285. doi:10.1002/(SICI)1097-461X(1997)64:3<285::AID-QUA2>3.0.CO;2-S
60. Amendola V, Boiocchi M, Fabbrizzi L, Palchetti A (2005) Chem Eur J 11:5648. doi:10.1002/chem.200500351
61. Morley JO (1996) J Mol Struct THEOCHEM 365:1. doi:10.1016/0166-1280(96)04492-2
62. Verbiest T, Houbrechts S, Kauranen M, Clays K, Persoons A (1997) J Mater Chem 7:2175. doi:10.1039/a703434b
63. Lambert C, Standlar S, Bourhill G, Brauchie C (1996) Angew Chem Int Ed Engl 35:644. doi:10.1002/anie.199606441
64. Abbotto A, Bradamante S, Facchetti A, Pagani GA, Ledoux I, Zyss (1998) J Metr Res Soc Symp Soc 488:819
65. Abbotto A, Beverina L, Bradamante S, Facchetti A, Klein C, Pagani GA, Wortmann R (2003) Chem Eur J 9:1991. doi:10.1002/chem.200204356
66. Qudar JL, Chemla DS (1977) J Chem Phys 66:2664. doi:10.1063/1.434213
67. Bhanuprakash K, Rao Laxmikanth (1999) J Chem Phys Lett 314:282. doi:10.1016/S0009-2614(99)01141-0
68. Abe J, Shirai Y (1997) J Phys Chem B 101:576. doi:10.1021/jp961711f
69. Yang GC, Su ZM, Qin CC, Zhao YH (2005) J Chem Phys 123:134302. doi:10.1063/1.2039707
70. Yang GC, Su ZM, Qin CC (2006) J Phys Chem A 110:4817. doi:10.1021/jp0600099
71. Yang GC, Liao Y, Su ZM, Zhang HY, Wang Y (2006) J Phys Chem A 110:8758. doi:10.1021/jp061286i
72. Yang GC, Guan W, Yan LK, Su ZM (2006) J Phys Chem B 110:23092. doi:10.1021/jp062820p
73. Yang GC, Shi SQ, Guan W, Fang L, Su ZM (2006) J Mol Struct THEOCHEM 773:9. doi:10.1016/j.theochem.2006.06.029